ME525 Applied Acoustics Lecture 17, Winter 2024
Impedances tubes and the Helmholtz resonator
The plane wave reflection coefficien

Peter H. Dahl, University of Washington

Impedance tubes and the Helmholtz resonator

Recall *specific acoustic impedance* expresses ratio of complex amplitude of harmonic acoustic pressure to acoustic velocity at some position $\vec{r}$ in the acoustic field, and *characteristic acoustic impedance* equals $\rho_n c_n$ for medium (or layer of medium) n; For specific acoustic impedance we need to understand more about the acoustic field, for example, if it is based on simple point source and spherical wave then specific acoustic impedance is a function of range r is

$$\frac{p(r)}{u_r(r)} = \frac{\rho_0 c}{1 + i/kr} \tag{1}$$

where the time dependence $e^{-i\omega t}$ cancels. If the acoustic field is plane wave then specific acoustic impedance equals characteristic acoustic impedance.

Recall that for two media with significantly difference characteristic acoustic impedances, say air and water, or air and cement wall, sound transmission between the two media will be reduced or completely prevented. Similarly, to encourage sound transmission, the impedances are made as close as possible and this is called impedance matching. (The word impedance comes from the Latin emphimpedire to hinder, or resist).

An impedance tube (Fig. 1) is common test device used in acoustic studies. A loudspeaker generates a harmonic tone of given frequency f. The purpose of the impedance tube is to measure the acoustic properties of the test sample shown on the left, such as acoustic absorbing material that might used in noise control applications. A microphone probe can slide back and forth and measure the pressure field at various distances from the test sample.
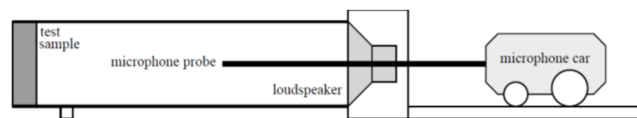

Figure 1: Impedance tube for measuring acoustic properties of test sample

The frequency f must satisfy $f < c/(1.71d)$ where d is the diameter of the tube (all units MKS). This means the frequency must be lower than the *cut-off frequency* of the tube. Let's postpone further discussion on this until our future lecture on modes, for now interpret this as only a plane wave for which the "ray" is aligned with the tube, can exist within the tube.
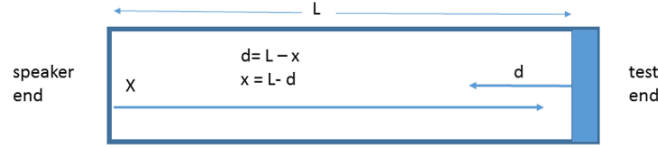
Figure 2: Coordinate system of impedance tube for measuring acoustic properties of test sample shown on the right at $x = d$.

Using the simplified diagram (Fig. 2) where the test material is now shown on the right and has unknown impedance Z_n. Model the acoustic pressure as follows:

$$p = Ae^{ikx} + Be^{-ikx} \tag{2}$$

where Ae^{ikx} represents a plane wave traveling to the right (positive x) in this coordinate system and Be^{-ikx} is a reflected plane wave traveling to the left, with harmonic time dependence of $e^{-i\omega t}$. Using Euler's equation the acoustic velocity (limited to x direction) is

$$u = \frac{A}{\rho c}e^{ikx} - \frac{B}{\rho c}e^{-ikx} \tag{3}$$

where ρc is the characteristic impedance of the acoustic media inside the tube, such as air. Interpret the first term as velocity directed towards the right, and the second as towards the left.

Now use fact that $x = L - d$ and after some rearrangement Eq. (1) is recast as:

$$p = Ae^{ikL}e^{-ikd} + Be^{-ikL}e^{ikd} \tag{4}$$

Next, recognize the incident pressure amplitude on the test sample at L (or at $d = 0$) equals Ae^{ikL}, and call this P. The reflected pressure is Be^{-ikL}, which we can call RP, where R is the reflection coefficient. The determination of the unknown R becomes one of the measurement goals. This gives

$$p(d) = P(e^{-ikd} + Re^{ikd}) \tag{5}$$

and similarly for acoustic velocity

$$u(d) = \frac{P}{\rho c}(e^{-ikd} - Re^{ikd}) \tag{6}$$

The specific acoustic impedance along the length of the tube as a function of distance d from the material is now given by

$$Z(d) = \rho c \frac{(e^{-ikd} + Re^{ikd})}{(e^{-ikd} - Re^{ikd})} \tag{7}$$

Observe that at $d = 0$ we get an equation for the impedance of an unknown test quantity Z_n, located

at $d = 0$

$$Z_n = Z(0) = \rho c \frac{(1 + R)}{(1 - R)} \tag{8}$$

It's useful to flip this around to arrive at expression for the reflection coefficient R as follows:

$$R = \frac{Z_n - \rho c}{Z_n + \rho c}. \tag{9}$$

This will be a recurring pattern that often comes up: where R equals the ratio of a combination impedance at the boundary (or "input impedance"), here Z_n, and impedance involving properties of the incident medium, here ρc.

Another result based on further manipulation of Eq. (6) that you should prove yourself is true is

$$Z(d) = \rho c \frac{Z_n - i\rho c \tan(kd)}{\rho c - i Z_n \tan(kd)} \tag{10}$$

The interpretation of Eq.(9) is as follows: the impedance "seen" by the sound source at distance d from the end of tube is combination of the end (or terminal) impedance, Z_n, plus the impedance contribution of the rest of the tube which has two ingredients, one the ρc of the tube media, and the other a combination of frequency and distance d along the tube which is embodied by the $\rho c \tan(kd)$ and $Z_n \tan(kd)$ terms. This idea is also directly linked with impedance translation theorem discussed later.

A simple example is a tube open or closed on one end (Fig. 3, left). For the open case, Then $Z_n = 0$ and Eq. (9) evaluated at $d = L$ goes to $Z(L) = -i\rho c \tan(kL)$, which equals 0 for values of $kL = \pi, 2\pi, 3\pi$, etc. Thus upon blowing lightly on one side of the tube, say a bit like blowing on a flute, the result would be range of frequencies. For frequencies such that the $L = n\lambda/2, n = 1, 2, 3....$ this will make the tube be "very accepting of sound", which happens when the tube length L equals multiples of $\lambda/2$. This is called an organ-pipe mode. You can try this yourself and find that very approximately the fundamental tone, or first harmonic, that result is such the frequency $\approx \frac{c}{2L}$.

The classic Helmholtz resonator (Fig. 3, right) can also be understood by appropriate combination of open and closed tube impedances in series. However, a more intuitive explanation is as follows (Rossing and Fletcher, 1994). Identify the vibrating air within neck of the "wine jug" bottle in Fig. 3 with a mass m, and volume of air in the captivity V as part of the spring system, where $m = \rho_0 S L$ and the spring constant $K = \rho_0 S^2 c^2 / V$.

Similar to any single degree of freedom mass-spring system, the resonance frequency is approximately equal to

$$f_{res} = \frac{c}{2\pi} \sqrt{\frac{S}{VL}} \tag{11}$$

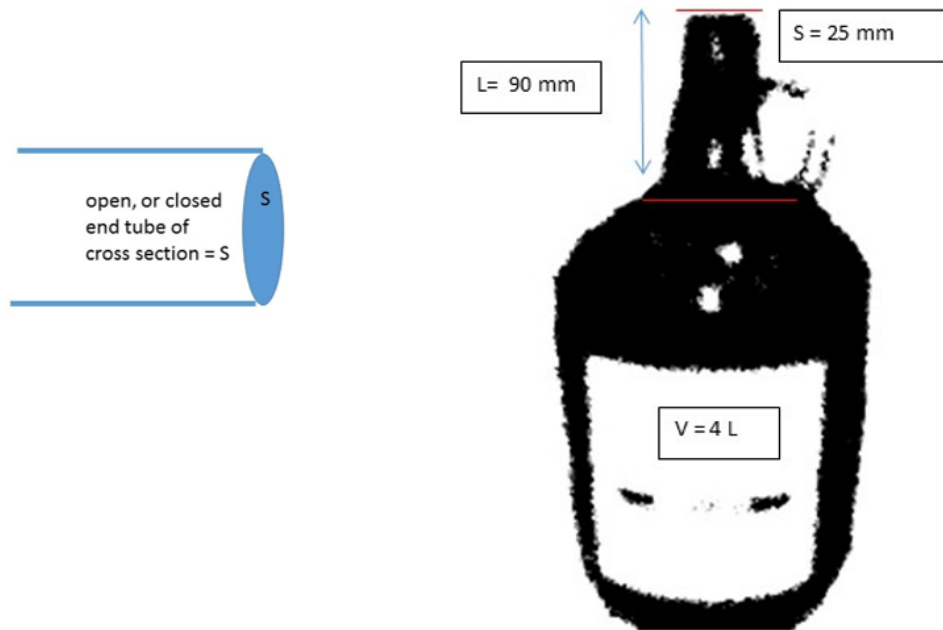Try blowing on a (preferably empty) bottle and impress your friends at a party!

Figure 3: Left: an open tube of length L with one end either open of close. Right: A Helmholtz resonator. Scales length L and volume V are as identified, note however that 25 mm identifies the diameter of the opening and not the opening area S which equals $\pi 0.0125^2$ m^2.

Plane waves and reflection

Plane waves are first discussed in Lecture 4 and its worth revisiting Eqs. (2-4) from that lecture. For spherical waves, e.g. radiation from a sphere of radius a with radial velocity u_r given on the boundary of this spherical source or the acoustic field described by the free space Green's function $g = \frac{e^{ikR}}{4\pi R}$ where $R = |\vec{r} - \vec{r}_0|$, with $\vec{r}$ representing the field point and $\vec{r}_0$ representing the source location. With spherical waves, the specific acoustic impedance, involved the non-dimensional parameter kr, and the region near the approximately delineated by $kr < 1$ is the hydrodynamic near field where pressure and velocity are 90° out of phase.

With plane waves the situation is quite different and many way simpler. The primary difference is that the specific acoustic impedance for plane waves equals the characteristic impedance, $\rho_0 c$, and the kinetic and potential energies are always equal, i.e., there this nothing analogous to the $kr < 1$ transition. However, plane waves are clearly a simplification, but at large ranges from a spherical source, $kr >> 1$, spherical waves behave like plane waves [e.g. again inspect Eq.(2) of Lecture 5]. However, despite this simplicity, the reflection plane waves from planar boundaries separating two different acoustic media provides the necessary building blocks for study of more complicated problems. Furthermore, the important problem of transmission of sound through such boundaries is also assessed by way of plane waves.

The situation is shown in Fig 4. A 2D plane wave is incident on the boundary between two

acoustic media at angle θ_0 with respect to the horizontal. (This is traditionally called a *grazing* angle. A completely equivalent description is by way of an *incident* angle with respect to the vertical. My preference is grazing angle.) The two acoustic media, now identified by subscripts 0 and 1, are described by their characteristic impedance, e.g, as in upper medium $\rho_0 c_0$. Later we can include more properties for each medium such as sound attenuation. (Note: obviously the need for subscripts 0,1,2, etc., for defining acoustic media, should not be confused with the small-valued ρ_1 used earlier to distinguish changes in acoustic density owing to the passage of a sound wave.)

This problem is fully described in the $x - y$ plane, with assumption that the boundary continues unimpeded in the z direction. Furthermore the boundary is assumed to exist from $x = -\infty$ to $x = +\infty$. Obviously this is a fiction, but the requirement is readily relaxed e.g., by an incident field consisting of a sound beam with finite extent incident on the surface, e.g. a finite-width sonar beam generated by a line array and studied with the Rayleigh integral. For now we stick with the idealization.

The incident plane wave acoustic field is

$$p_{inc}(x,y) = Ae^{ik_0 x \cos\theta_0 - ik_0 y \sin\theta_0} \tag{12}$$

where A is an amplitude, providing a dimension of pressure, but otherwise is of no importance. The subscript 0 identifies wavenumber k_0 and angle θ_0 linked to the incident medium. (As before, time dependence is assumed to be $e^{-i\omega t}$ which we leave out the problem as it plays no role.) Figure 4 shows some phase fronts (separated by λ) representative of the incident plane wave field. After this we'll stop drawing the phase fronts as the key property is the *ray* or direction normal the phase fronts as described by angle θ_0.

Boundary conditions: continuity of acoustic pressure and normal velocity

This problem involves a reflected and transmitted complex acoustic field, where the reflected field is

$$p_{ref}(x,y) = RAe^{ik_0 x \cos\theta_0 + ik_0 y \sin\theta_0} \tag{13}$$

and transmitted field in the lower medium is

$$p_{trans}(x,y) = TAe^{ik_1 x \cos\theta_1 - ik_1 y \sin\theta_1} \tag{14}$$

and where the subscript 1 identifies wavenumber k_1 and angle θ_1 linked to the lower medium.

Our goal is to find the reflection coefficient R and transmission coefficient T, through analysis of two essential continuity conditions along the boundary separating the two acoustic media. These two conditions, continuity of acoustic pressure and normal velocity, formally specify the boundary conditions for solving the problem, and are worth memorizing.
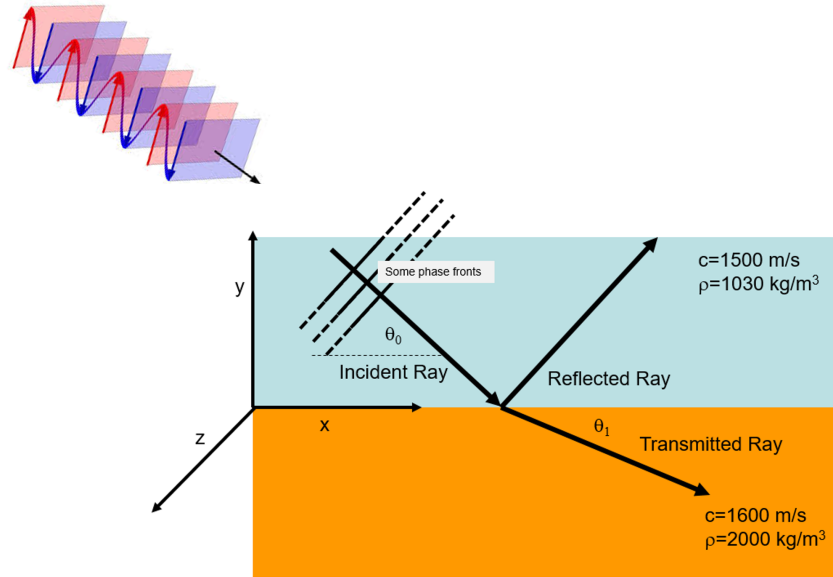
Figure 4: Main figure: A 2-D plane wave encountering a boundary between two acoustic media, sea water above the sea bed below. The incident plane wave acoustic field in the upper medium has propagation angle θ_0, as depicted by the corresponding ray. A reflected and transmitted field, with propagation angle θ_1 are also symbolized by corresponding rays. Upper left: depiction of a 3D plane wave and corresponding ray (black arrow).

The first boundary condition is *continuity of pressure* across the boundary. That is, the pressure must be continuous across the boundary to preserve the immobility of the boundary, e.g., if there existed a pressure difference then the boundary would be accelerated in one direction or the other. This condition requires $p_{inc}(x,0) + p_{ref}(x,0) = p_{trans}(x,0)$, which leads to

$$(1+R)e^{ik_0 x \cos\theta_0} = Te^{ik_1 x \cos\theta_1} \tag{15}$$

To make each side equal over all values of x requires a *continuity of phase* or

$$k_0 \cos\theta_0 = k_1 \cos\theta_1 \tag{16}$$

This leads to one of the most important laws in acoustics and wave propagation, known as *Snell's Law*. For the specification of θ_0, θ_1 in Fig. 1, Snell's laws is therefore expressed as

$$\frac{\cos\theta_0}{c_o} = \frac{\cos\theta_1}{c_1} \tag{17}$$

It pays to memorize Snell's law–and I like the form of Eq.(16) involving grazing angle with respect to the horizontal and cosine, rather than incident angle and sine. Upon application of Snell's law we get

$$1 + R = T. \tag{18}$$

Closer inspection of how the angles work (Fig. 4), it should be evident that upon entering a region of differing sound speeds, a ray will bend, or refract, towards the lower speed with the change in angle governed by Snell's law. It pays to memorize: rays always want to bend, or refract, towards the region of lower sound speed.

The second continuity/boundary condition is continuity of normal acoustic velocity u_n at the boundary. Apply Euler's equation to find u_n and get

$$\frac{1}{i\omega\rho_0}\frac{\partial p_{inc} + p_{ref}}{\partial y}\Big|_{y=0} = \frac{1}{i\omega\rho_1}\frac{\partial p_{trans}}{\partial y}\Big|_{y=0} \tag{19}$$

where ρ_1 is the background density for the lower medium. The frequency ω cancels, and upon applying Snell's law we arrive at

$$\frac{\sin\theta_0}{\rho_0 c_0}(1 - R) = \frac{\sin\theta_1}{\rho_1 c_1}T \tag{20}$$

Now put $Z_0 = \frac{\rho_0 c_0}{\sin\theta_0}$ and $Z_1 = \frac{\rho_1 c_1}{\sin\theta_1}$, and find

$$R(\theta_0) = \frac{Z_1 - Z_0}{Z_1 + Z_0} \tag{21}$$

where the reflection coefficient is a function of θ_0, as in $R(\theta_0)$ with θ_1 determined from Snell's law. Notice the analogy with Eq. (9) involving the impedance tube problem.

The Z are impedance quantities and you should recognize the characteristic impedances of the two media $\rho_0 c_0$ and $\rho_1 c_1$, each divided by $\sin$ of the incoming θ_0 or transmitted θ_1 grazing angle. These impedances are referred to as *normal specific acoustic impedance* (Frisk, 1994), given their relation to the acoustc velocity normal to the boundary.

Quick check: In the case of plane wave impinging on the air-water interface from below, expect Z_0 representing the water medium will be $|Z_0| >> |Z_1|$ representing the air medium. Thus $R \approx -1$; this is close enough such that $R = -1$ is *standard practice* for representing the boundary condition between water and air for modeling underwater sound. Similarly, sound impinging on an air-water boundary from above, will have $|Z_0| << |Z_1|$ and thus $R \approx 1$. These two cases for which all the incident acoustic energy is reflected, insofar as $|R| = 1$ for all angles θ_0, and no acoustic energy enters the lower medium, are known as *impenetrable boundaries* (Frisk, 1994). There can, in fact, be some small degree of acoustic penetration across the boundary as you may have experienced yourself while detecting air-borne sound while swimming underwater.

The critical angle

Inspect now closely the relation between incident (θ_0) and transmitted (θ_1)angles in the reflection process (Fig. 4), as governed by Snell's Law in Eq. (16). The reflected angle, although not shown, also is θ_0 for *specular reflection* (Frisk, 1994) from a flat interface. Observe from Snell's law

that as θ_0 is reduced so too is θ_1. Eventually when θ_0 reaches the *critical angle*, then θ_1 equals $0°$ and the transmitted field is propagating along the boundary. Define formally the critical angle θ_c as

$$\cos \theta_c = \frac{c_0}{c_1} \tag{22}$$

which is a basic, combined property of the two acoustic media involved in the reflection.

For example, with the sound speeds given in Fig. 4 the critical angle $\theta_c = 20.4°$ which is a typical critical angle for seawater to seabed reflection. Softer, mud-like sediments will have a lower speed, and therefore a lower θ_c, harder rock-like sediments will have a higher sound speed and thus higher θ_c. In the field of diagnostic ultrasound, one may be interested in the critical angle for transmission from a soft-tissue medium ($c_0 \approx 1500$ m/s) to bone ($c_1 \approx 3000$ m/s), which puts $\theta_c = 60°$.

Using the again the geometry of Fig. 4, the reflection process plotted in the form of $R(\theta_0)$ is shown two different lower media (Fig. 5). The lower media differ only in terms of sound speeds; one a "harder" seabed (speed 1800 m/s) and the other a "softer" seabed (speed 1540 m/s). For this demonstration the densities for each are the same 1800 kg/m^3, but more realistically we would expect the medium with higher sound speed to have a slightly density. However the key difference to observe is the large change in critical angle. For grazing angles less than θ_c, $R(\theta_0)$ is complex with $|R|$ equal to 1. This angular region is called *total internal reflection*, for which no sound energy can be effectively transmitted into the lower medium. For $\theta_0 > \theta_c$, $R(\theta_0)$ transitions to a real-value for with $|R| < 1$.

At very high grazing angles approaching $90°$, or normal incidence, the value of $R(\theta_0)$ depends on the combination and ratio of the characteristic impedances of the two media as follows

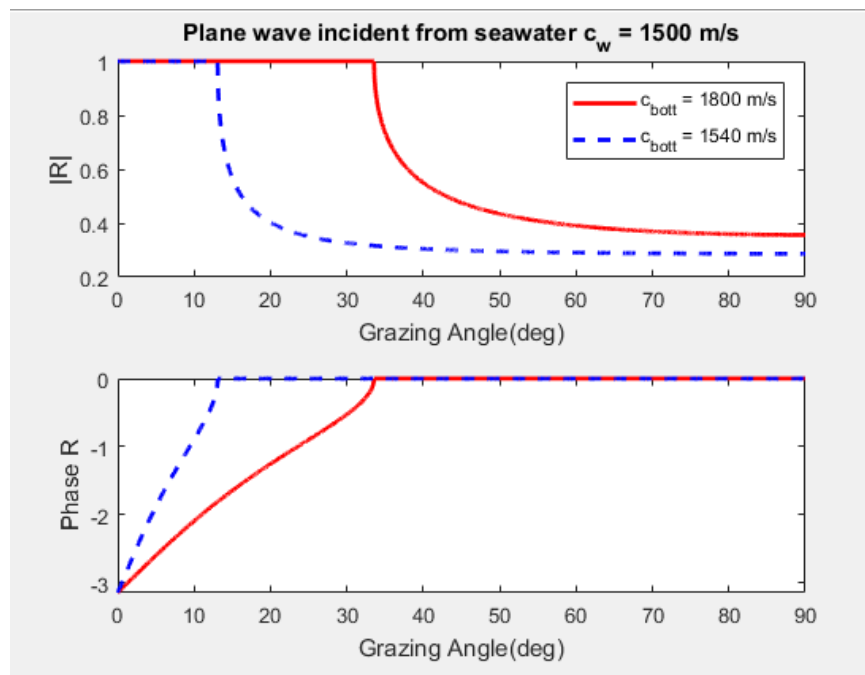$$R \approx \frac{\rho_1 c_1 - \rho_0 c_0}{\rho_1 c_1 + \rho_0 c_0}. \tag{23}$$

Figure 5: $|R|$ and phase of R as function of grazing angle θ_0 for water-sediment reflection. Two sediments shown with differing sound speeds. The densities for each sediment case is 1800 m/kg^3, and water density is 1025 m/kg^3.

References

T. D. Rossing and N. H. Fletcher, *Principles of Vibration and Sound*, (Springer, New York, 1994)

]G. V. Frisk, *Ocean and Seabed Acoustics* (Prentice Hall, Englewood Cliffs, NJ, 1994)

L. E. Kinsler, A. R. Frey, A. B. Coppens, and J. V. Sanders, *Fundamentals of Acoustics*, (John Wiley & Sons, New York, 1980)

ME525 Applied Acoustics Lecture 18, Winter 2024
The plane wave reflection coefficient and Snell's Law

Peter H. Dahl, University of Washington

Plane waves and reflection
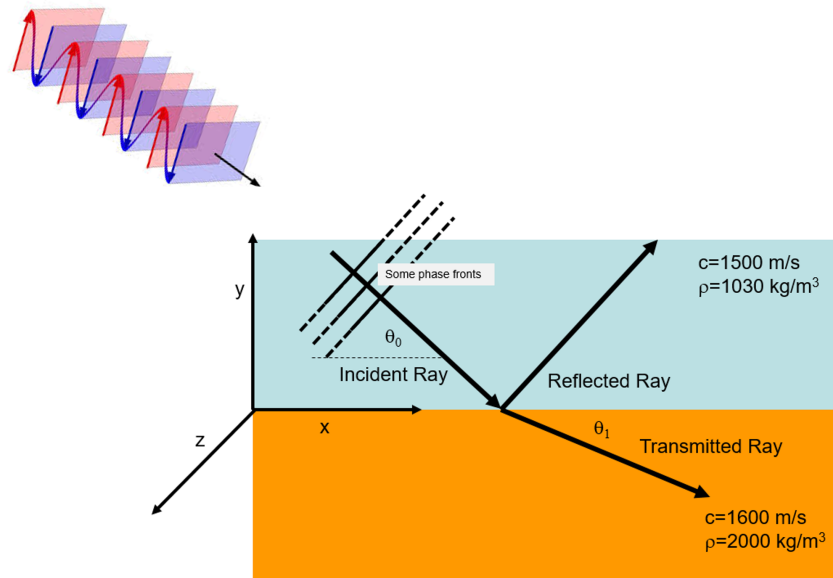
Figure 1: Main figure: A 2-D plane wave encountering a boundary between two acoustic media,sea water above the sea bed below. The incident plane wave acoustic field in the upper medium has propagation angle θ_0, as depicted by the corresponding ray. A reflected and transmitted field, with propagation angle θ_1 are also symbolized by corresponding rays. Upper left: depiction of a 3D plane wave and corresponding ray (black arrow).

The critical angle

The relation between incident (θ_0) and transmitted (θ_1)angles in the reflection process (Fig. 1), is governed by Snell's Law

$$\frac{\cos \theta_0}{c_o} = \frac{\cos \theta_1}{c_1}.$$ (1)

The reflected angle, although not shown, equals θ_0 for *specular reflection* (Frisk, 1994) from a flat interface. Importantly, observe from Snell's law that as θ_0 is reduced so too is θ_1. Eventually when θ_0 reaches the *critical angle*, then θ_1 equals $0°$ and the transmitted field is propagating along the boundary. Define formally the critical angle θ_c as

$$\cos \theta_c = \frac{c_0}{c_1}$$ (2)

which is a basic, combined property of the two acoustic media involved in the reflection.

For example, with the sound speeds given in Fig. 1 the critical angle $\theta_c = 20.4°$ which is a typical critical angle for seawater to seabed reflection. Softer, mud-like sediments will have a lower speed, and therefore a lower θ_c, harder rock-like sediments will have a higher sound speed and thus higher θ_c. In the field of diagnostic ultrasound, one may be interested in the critical angle for transmission from a soft-tissue medium ($c_0 \approx 1500$ m/s) to bone ($c_1 \approx 3000$ m/s), which puts $\theta_c = 60°$.

Using the again the geometry of Fig. 1, the reflection process plotted in the form of $R(\theta_0)$ is shown for two different lower media (Fig. 2). The lower media differ only in terms of sound speeds; one a "harder" seabed (speed 1800 m/s) and the other a "softer" seabed (speed 1540 m/s). For this demonstration the densities for each are the same 1800 kg/m^3, but more realistically we would expect the medium with higher sound speed to have a slightly density. However the key difference to observe is the large change in critical angle. For grazing angles less than θ_c, $R(\theta_0)$ is complex with $|R|$ equal to 1. This angular region is called *total internal reflection*, for which no sound energy can be effectively transmitted into the lower medium. For $\theta_0 > \theta_c$, $R(\theta_0)$ transitions to a real-value for with $|R| < 1$.

The acoustic field in the lower medium (seabed in this example) is also very interesting. We do not have time to pursue further in this course but details are provided in the Appendix to this lecture.

At very high grazing angles approaching $90°$, or normal incidence, the value of $R(\theta_0)$ depends on the combination and ratio of the characteristic impedances of the two media as follows

$$R \approx \frac{\rho_1 c_1 - \rho_0 c_0}{\rho_1 c_1 + \rho_0 c_0}. \tag{3}$$

Another view of Snell's law using the trace wavelength

Figure 3 shows a ray of angle θ_0 within a medium characterized by sound speed c_0, incident on boundary below which the sound speed has changed to c_1, with $c_1 > c_0$. Phase fronts separated by λ_0 in the upper medium must *match* those separated by λ_1 in the lower medium: this gives rise to Snell's Law, and shows how a ray in faster medium must bend or refract towards the slower medium, and the opposite will occur if $c_1 < c_0$. The sound frequency determines λ_0 and λ_1, and projections of these wavelengths onto the boundary establishes a *trace wavelength* λ_t.

Bottom loss

Bottom loss is defined as $20 \log_{10} |R(\theta)|$ where θ is the bottom grazing angle, to be associated with ray that reflects from the bottom. We have have more details to discuss about ray theory, but suffice to say that everything is essentially governed by Snell's law. A program for computing rays
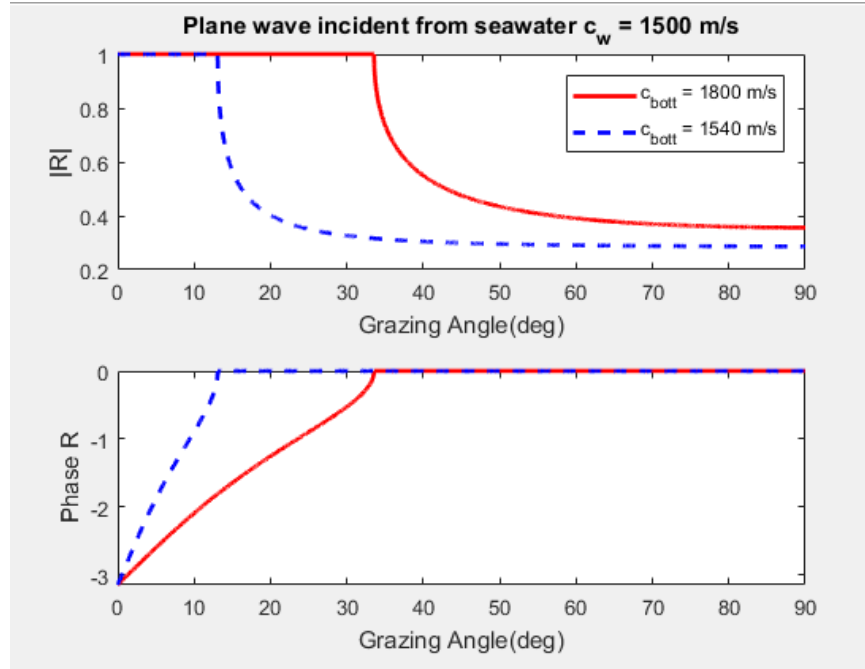
Figure 2: $|R|$ and phase of R as function of grazing angle θ_0 for water-sediment reflection. Two sediments shown with differing sound speeds. The densities for each sediment case is 1800 m/kg^3, and water density is 1025 m/kg^3.
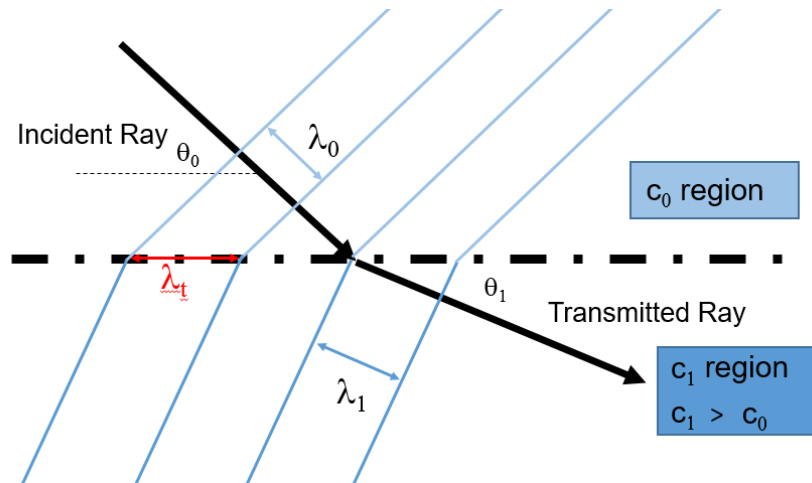

Figure 3: Illustrating the projection of a plane wave in region of sound speed c_0 onto a boundary separating region with sound speed c_1, where $c_1 > c_0$. The sound frequency determines λ_0 and λ_1, projections of these onto the boundary establishes a trace wavelength λ_t leading to Snell's law $\frac{\cos\theta_0}{c_0} = \frac{\cos\theta_1}{c_1}$. Ultimately frequency is not a driver in Snell's law as wavelengths will scale accordingly.

will "launch" a ray at the sound source at angle θ, (with respect to horizontal in my preferred convention) and such a ray continues moving forward at angle θ until either a boundary is encountered in which case it reflects and $\theta \to -\theta$, or the ray enters a new sound speed regime with θ changing, or the ray refracts, according to Snell's law.

Figure 4 shows a series of ray diagrams that trace rays launched from a receiver within a spec-

ified angular width, with rays governed as just described towards a receiver at some fixed range. The rays are computed following the ocean sound speed profilen (left panel) which has sound speed generally decreasing with increasing depth. This larger set of rays is known as a *ray fan*. A subset of thes rays reach the target location (within some tolerance) and these are called *eigenrays*.
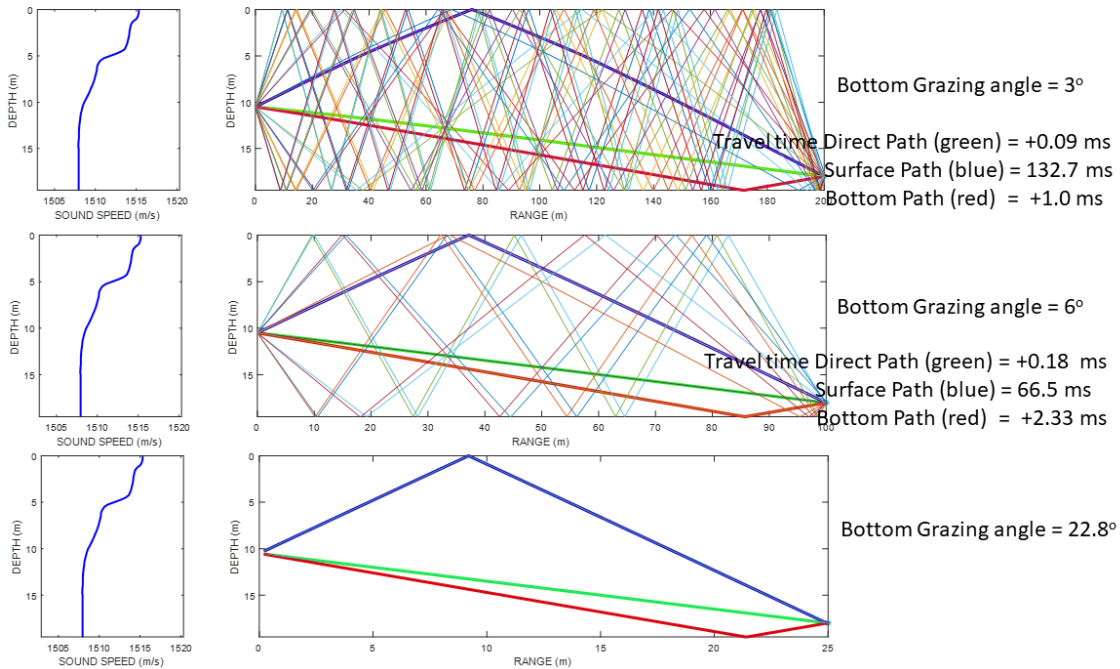

Figure 4: Ray theory travel and bottom grazing angle study for three ranges, based on source depth at 10 m, receiver depth at 17 m, and sound speed profile shown on the left. The cases at range 200 and 100 m show rays of different angles "launched" from the source. A few of these rays reach the target depth at the specified range (within some tolerance). These are called eigenrays. The grazing angle for the eigenray that reflects from the seabed once is shown for each case.

Figure 5 shows an ocean sound speed profile (a) and an eigenray diagram (b), i.e., only the subset of rays that connext source and receiver points based on this sound speed profile. Notice the large change in sound speed from about 30 m to the sea surface over which the speed increases by about 40 m/s, due to the presence of a *thermocline*.

The eigenrays can be named according to how they interact with the sea surface and seabed boundaries, as in S: surface path, D: direct path, B: bottom path, BS: bottom-surface path, SB: surface-bottom path, and SBS: surface-bottom-surface path. Panels (c) and (d) show time series of the received pulse (x axis is time in relative units), plotted in dB. The different arrivals, as in D (direct), S (surface path), etc. are easily identified in the data. For example, the B-path has a grazing angle on the bottom of about $26°$, and the data are consistent with a bottom loss of about 2.5 dB.

Figures 6 and 7 show examples of bottom loss data from field experiments. Such data is often subject to high degree of variation due to many factors: changing water conditions, small changes in measurement geometry as ship moves around, etc. However we are generally able to capture
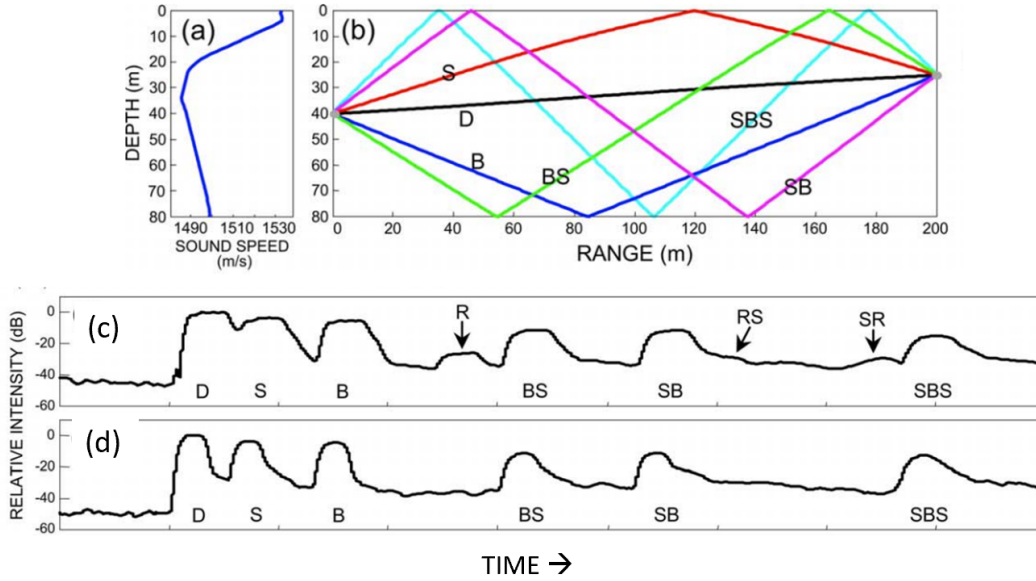
Figure 5: From the study by Choi, Dahl and Goff (2008) showing eigenrays between source at depth 40 m and receiver at depth 30 m, separated by 200 m. Sound speed profile (a) is used to compute eigenrays (b) that are coded according to S: surface path D: direct path B: bottom path BS: bottom-surface path SB: surface-bottom path SBS: surface-bottom-surface path.

(c) and (d) time series of the received pulse (x axis is time in relative units), plotted in dB. The different arrivals, as in D (direct), S (surface path), etc. are identified. Note that plot (d) corresponds to the eigenrays shown; plot (c) is a result of a different source and receiver geometry.

a sense of the data with simple modeling of $R(\theta)$ or $20 \log_{10} |R(\theta)|$ using a model where $Z_0 = \frac{\rho_0 c_0}{\sin \theta_0}$ and $Z_1 = \frac{\rho_1 c_1}{\sin \theta_1}$, and find

$$R(\theta_0) = \frac{Z_1 - Z_0}{Z_1 + Z_0}. \tag{4}$$

However Eq.(4) represents the simplest of all models where the lower medium is described by $\rho_1 c_1$ and continues forever. In other words, the lower medium is a mathematical *half-space*.

Things change if, for example, after some layer depth H the sound speed takes on a change from c_1 to c_2, with layering producing oscillations in $R(\theta)$ not seen in the form of Eq.(4). There are some relatively simple ways to accommodate this layering using the Impedance Translation Theorem, to be discussed next.
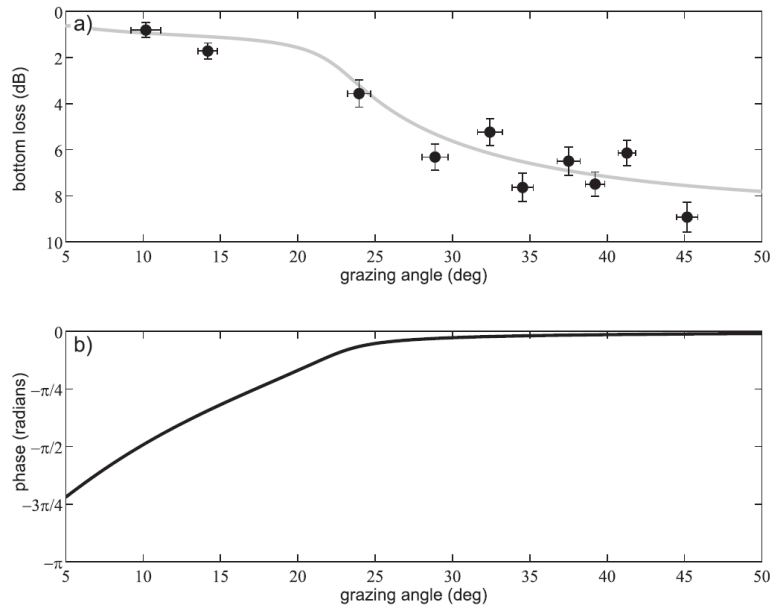
Figure 6: Measurements of bottom loss defined as $20 \log_{10} |R(\theta)|$ from a study by Dall'Osto, Choi and Dahl, 2017.
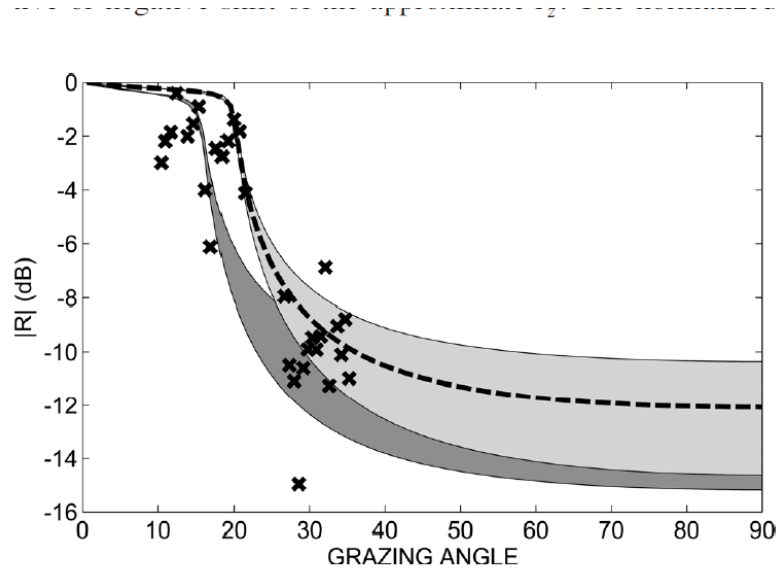

Figure 7: Measurements of bottom loss defined as $20 \log_{10} |R(\theta)|$ from a study by Dall'Osto, Dahl and Choi, 2012

Appendix:

The evanescent field for $\theta_0 < \theta_c$, inhomogeneous plane waves

For angles greater than θ_c, or 20.3° for the case of Fig. 1, there is a transmitted angle θ_1 in the lower medium that we easily find through Snell's law. What happens for $\theta_0 < \theta_c$? Notice that for $\theta_0 < \theta_c$, then $\cos \theta_1 = \frac{c_1}{c_0} \cos \theta_0$ cannot be satisfied a real-valued angle θ_1, since $\frac{c_1}{c_0} \cos \theta_0 > 1$, and the

angle θ_1 must instead be complex. We find it this way:

$$\sin \theta_1 = \sqrt{1 - \cos^2 \theta_1} = i\sqrt{(\frac{c_1}{c_0} \cos \theta_0)^2 - 1} \tag{5}$$

To understand this new kind of angle, consider the transmitted field in medium 1

$$p_{trans}(x, y) = TAe^{ik_1 x \cos \theta_1 - ik_1 y \sin \theta_1} \tag{6}$$

which applies only for $y < 0$ and where constant A used to put the dimension to pressure, but it is otherwise not essential. Substitute now the imaginary $\sin \theta_1$ from Eq.(2) and invoke Snell's law to replace $k_1 x \cos \theta_1$ (as that relation must continue to hold) and the expression for p_{trans} becomes

$$p_{trans}(x, y) = TAe^{ik_0 x \cos \theta_0 + k_1 y \sqrt{(\frac{c_1}{c_0} \cos \theta_0)^2 - 1}} \tag{7}$$

with exponential decay in the y direction (noting $y < 0$).

Equation (7) represents a plane known as an *inhomogeneous* plane wave (Frisk, 1994) because there is propagation in one (x) direction and exponential decay in the other (y) direction. Another term often used is that the acoustic field is *evanescent* in the y direction. For example, airborne sound heard while one is swimming underwater but still close to the surface has likely reached you via this evanescent wave.
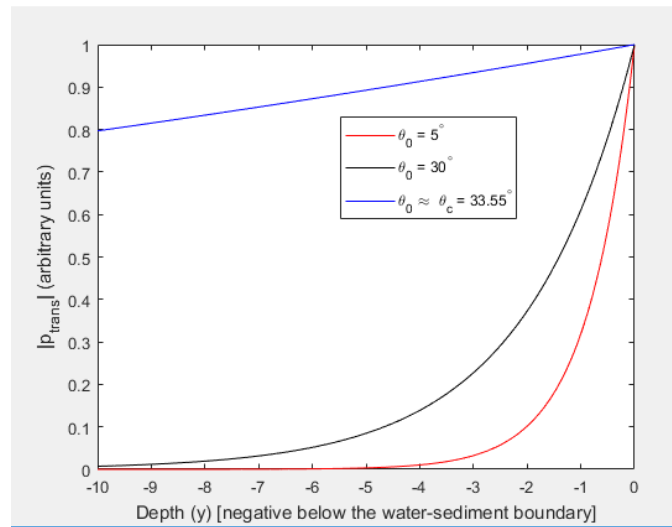

Figure 8: Showing changes in exponential decay for three grazing angles cases less than or approximately equal to the critical angle. For clarity, magnitude of the transmitted fields are plotted as normalized by maximum value at the water-sediment boundary.

The decay of transmitted field p_{trans} for three cases, defined by grazing angles less than or approximately equal to the critical angle is shown in Fig 8. For this example, the critical angle equals $33.55°$, representing the reflection from a plane wave incident from sea water medium (1500 m/s) onto seabed medium (speed 1800 m/s). Observe that the decay is greatest for smallest grazing angle ($5°$) below the critical angle, where as for a grazing angle very near critical the decay rate is less.

References

Frisk, G. V. *Ocean and Seabed Acoustics* (Prentice Hall, Englewood Cliffs, NJ, 1994)

ME525 Applied Acoustics Lecture 19, Winter 2024
Impedance Translation Theorem

Peter H. Dahl, University of Washington

Plane wave reflection from a layered seabed

The problem of finding the plane wave reflection coefficient R from a layered boundary (Fig. 1) is easily solved with the *impedance-translation theorem* (Brekhovskikh, 1980; Pierce 1989).
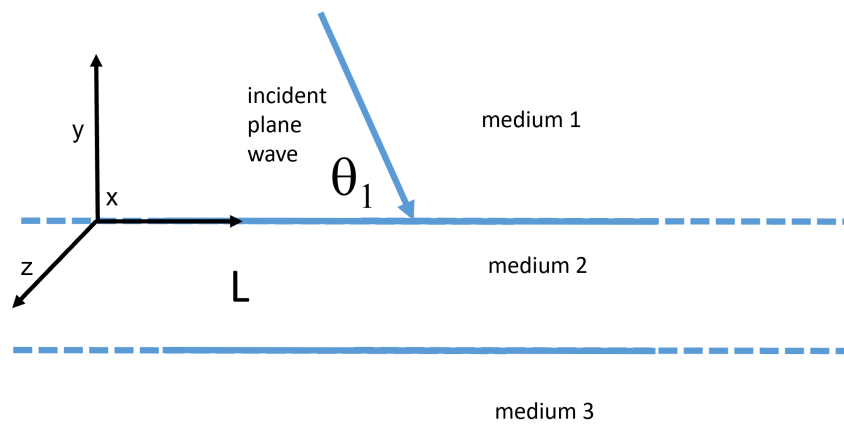

Figure 1: Geometry from reflection from a layered media at arbitrary grazing angle, θ_1. A layer of thickness L extends from $y = 0$ to $y = -L$.

To get a sense of how this simplifies the problem, consider first solving the problem by invoking standard boundary conditions of continuity of pressure, and normal (vertical) velocity at each of the interfaces. For this take the incident field in medium 1 as

$$p_{inc}(x, y) = e^{ik_1 x \cos \theta_1 - ik_1 y \sin \theta_1} \tag{1}$$

(for simplicity set coefficient A equal to 1.) In medium 2 (the layer) we must have both up and down going fields, and let those coefficients be, A and B, respectively. In medium 3 there is only one field with coefficient out front equal to T.

Next apply the two boundary conditions, where θ_1 is grazing angle for the incidence field. The boundary conditions at $y = 0$ and $y = L$ are that continuity of pressure requires

$$1 + R = A + B, \quad y = 0$$

$$Ae^{ik_2 L \sin \theta_2} + Be^{-ik_2 L \sin \theta_2} = Te^{ik_3 L \sin \theta_3}, \quad y = -L$$

where R and T are the reflection and transmission coefficients, and continuity of normal velocity requires

$$\sin\theta_1(1-R)/(\rho c)_1 = \sin\theta_2(A-B)/(\rho c)_2, \quad y=0$$

$$\sin\theta_2(Ae^{ik_2L\sin\theta_2} - Be^{-ik_2L\sin\theta_2})/(\rho c)_2 = \sin\theta_3 Te^{ik_3L\sin\theta_3}/(\rho c)_3, \quad y=-L$$

There appears four equations with four unknowns, R, T and A, B, which is solvable say by setting up a 4 by 4 matrix to recover unknowns R and T. But let's instead exploit the impedance-translation theorem.

For a layer of length L characterized by medium 2, identify:

$$Z_{layer} = (\rho c)_2/\sin\theta_2$$

$$k_{layer} = k_2\sin\theta_2$$

and for medium 3 below identify:

$$Z_{load} = (\rho c)_3/\sin\theta_3$$

We can roughly interpret Z_{layer} as the impedance of the "transmission line" connecting the medium 1 and medium 3. We can interpret Z_{load} as load or terminal impedance for this system. That is, sound can reflect upward at the interface between medium 2 and 3, but any sound actually entering into medium 3 is not coming back, hence terminal impedance.

Next compute a new Z_{in} as follows:

$$Z_{in} = Z_{layer}\frac{Z_{load} - iZ_{layer}\tan(k_{layer}L)}{Z_{layer} - iZ_{load}\tan(k_{layer}L)} \tag{2}$$

where the Z_{in} stands for input impedance. Of course, care is needed in computing the angles θ_1 going to θ_2 and finally to θ_2. Snell's law does this which in this case means:
$k_1\cos\theta_1 = k_2\cos\theta_2 = k_3\cos\theta_3$
and angles can in general be complex.

We find Z_{in} for this problem–almost by inspection–as follows:

$$Z_{in} = [(\rho c)_2/\sin\theta_2]\frac{[(\rho c)_3/\sin\theta_3 - i[(\rho c)_2/\sin\theta_2]\tan(k_2\sin\theta_2 L)]}{[(\rho c)_2/\sin\theta_2 - i[(\rho c)_3/\sin\theta_3]\tan(k_2\sin\theta_2 L)]} \tag{3}$$

Having found Z_{in}, the plane wave reflection coefficient R from layered medium at arbitrary grazing angle is then

$$R = \frac{Z_{in} - (\rho c)_1/\sin\theta_1}{Z_{in} + (\rho c)_1/\sin\theta_1} \tag{4}$$

Note: compare this equation with Eq.(4) of Lecture 18 representing plane wave reflection from two halfspaces, characterized by upper medium 0 (Z_0), and lower medium 1 (Z_1). Be mindful that I have now changed to three indices to represent upper, layer and lower media as follows: 1 for the medium through which the wave initially travels, 2 for the layer, and 3 for the medium into which the wave is transmitted.

As an example, put:

medium 1 $\rho = 1025$ kg/m^3, $c = 1500$ m/s
medium 2 $\rho = 1400$ kg/m^3, $c = 1600$ m/s
medium 3 $\rho = 2000$ kg/m^3, $c = 1900$ m/s

and set layer L equal to 50 and 5 m. The result (Fig. 2) for $|R|$ as a function of grazing angle shows a strong dependence on layer thickness L, which translates to a frequency dependence. The black,dashed line forms kind of envelope of $|R|$ and is based on the reflection from a halfspace of medium 3, i.e, setting $L = 0$.
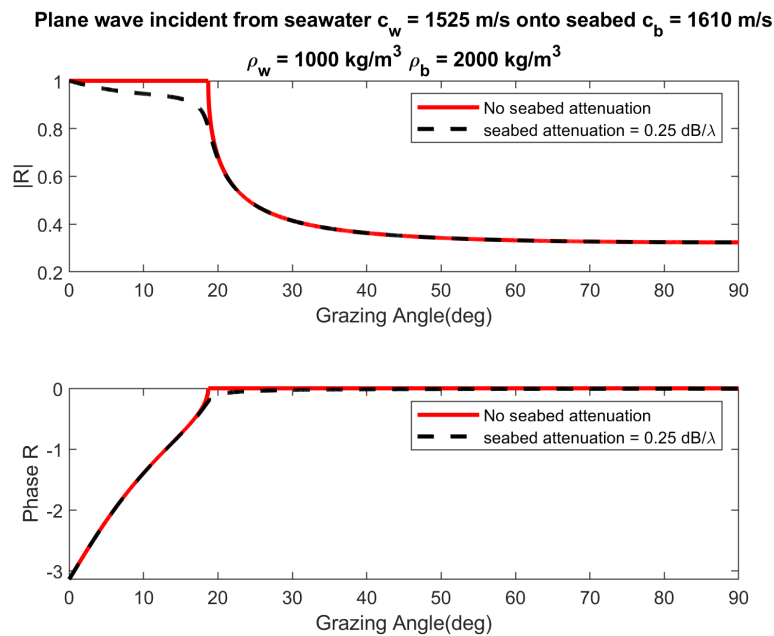

Figure 2: Magnitude of the plane reflection coefficient $|R|$ from a layered seabed as function of grazing angle.

With the $L = 50$ m case there is strong interference pattern set up by waves trapped within the layer. Using the wavenumber for the layer $k_2 = \frac{2\pi 200}{1600}$, then $k_2 L \sim 39$. With the $L = 5$ m case, $k_2 L \sim 3.9$; we anticipate that the influence of the layer diminishes as $k_2 L$ is reduced to a value of ~ 1 or less. I experimented just a bit and when $k_2 L \sim 0.5$, the effect of the layer is nearly gone and reflection is as if it is from the halfspace.

The idea of identifying an input impedance Z_{in}, such as for the layer and halfspace in the region $x > 0$, is a very powerful one, and the procedure is easily extended for multiple layers. For example,

for the case of two layers L_1 and L_2 a new load impedance Z_{load} is constructed for based on the combination of the lowest layer impedance and the terminal impedance. This becomes the load impedance for the layer directly above, and so on. More discussion on the extension to n layers can be found in Brekhovskikh (1980).

The single expansion chamber muffler

The impedance translation theorem is not limited to problems on reflections from layered media, but finds all manner of applications in linear system theory. The following is example involving sound propagation within a confined tube of varying cross section (Fig. 3), representing a a single expansion chamber muffler with many applications in terms of noise control, such as a car muffler.
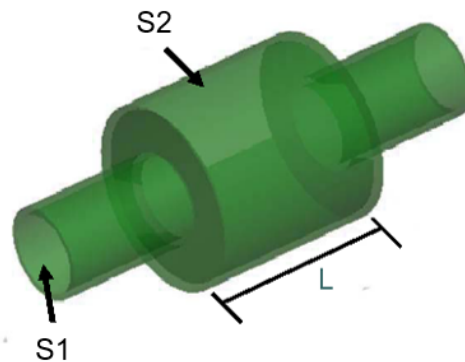

Figure 3: Single expansion chamber muffler with input area $S1$, expanding to area $S2$ for length L, then returning to area $S1$.

The geometry and acoustic fields for the problem are shown in Fig. 4, where we assume a plane wave is incident at $x = 0$. The plane wave direction, or ray, is confined to be parallel with the tube. As such, the plane wave must have a frequency satisfying $f < \frac{c}{1.7d}$, where d is the largest diameter of the muffler. If $f < \frac{c}{1.7d}$ is satisfied, it said that the muffler supports a a single axial mode as described by plane with "ray" pointing straight down the tube (e.g. as in Fig. 1 of Lecture 4).

The pressure and velocity boundary conditions are analogous to those that we've encountered in the context of reflection from layered media. However with the change in area at $x = 0$ and $x = L$ we now require continuity of volume velocity, or area times velocity (Pierce, 1989). Continuity of pressure requires

$$1 + R = A + B, \quad x = 0$$
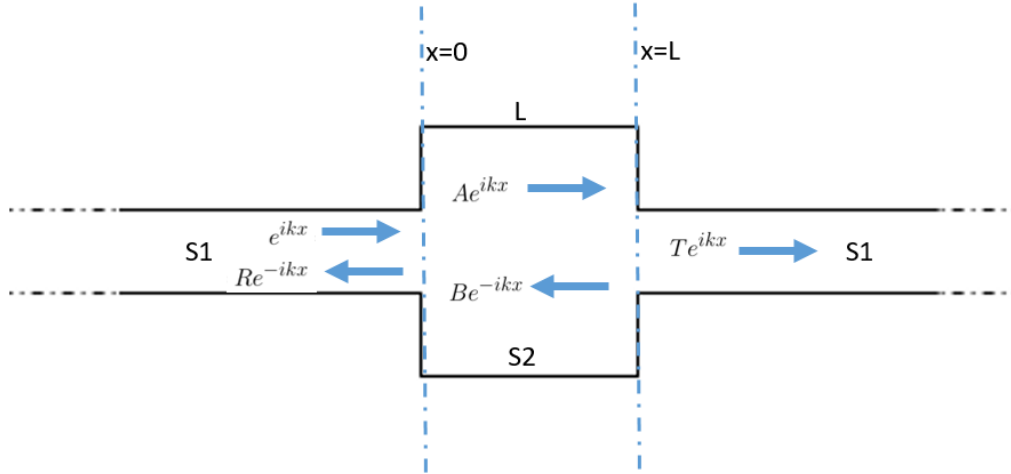$$Ae^{ikL} + Be^{-ikL} = Te^{ikL}, \quad x = L$$

Figure 4: The geometry and acoustic fields for the problem for single expansion chamber muffler with input area $S1$, expanding to area $S2$ for length L, then returning to area $S1$.

where R and T are the reflection and transmission coefficients, while continuity of volume velocity requires

$$S1(1 - R)/(\rho c) = S2(A - B)/(\rho c), \quad x = 0$$
$$S2(Ae^{ikL} - Be^{-ikL})/(\rho c) = S1Te^{ikL}/(\rho c), \quad x = L$$

These are summarize in the matrix equation involving matrix

$$M = \begin{pmatrix} 1 & 0 & -1 & -1 \\ -S1 & 0 & -S2 & S2 \\ 0 & -e^{ikL} & e^{ikL} & e^{-ikL} \\ 0 & -S1e^{ikL} & S2e^{ikL} & -S2e^{-ikL} \end{pmatrix} \tag{5}$$

$$C = \begin{pmatrix} -1 \\ -S1 \\ 0 \\ 0 \end{pmatrix} \tag{6}$$

$$P = \begin{pmatrix} R \\ T \\ A \\ B \end{pmatrix} \tag{7}$$

Find the unknown vector $P = M^{-1}C$, with reflection coefficient $R = P(1)$ and transmission coefficient $T = P(2)$. Go ahead, try it.

Or, why not try a the more simpler approach using the impedance translation theorem? To do so, find the input impedance Z_{in} of the single expansion chamber muffler system. Identify:

$$Z_{layer} = \rho c / S2$$

$$k_{layer} = k$$

$$Z_{load} = \rho c / S1$$

Following the prescription of Eq.(2) then find Z_{in} as follows:

$$Z_{in} = \frac{\rho c}{S2} \left[\frac{\frac{\rho c}{S1} - i \frac{\rho c}{S2} \tan(kL)}{\frac{\rho c}{S2} - i \frac{\rho c}{S1} \tan(kL)} \right] \tag{8}$$

and immediately arrive at expression for the reflection coefficient

$$R = \frac{Z_{in} - Z_0}{Z_{in} + Z_0} \tag{9}$$

where $Z_0 = \rho c / S1$.

To study the noise reduction performance of this muffler, there are two key approaches, one is called *insertion loss* requiring finding the sound pressure level (in dB) before insertion of the device, then find the drop in this level after insertion of the muffler (Pierce, 2008). Insertion loss is easy to measure. The other is called *transmission loss*, or TL representing the ratio of incident to transmitted acoustic power and is usually expressed in decibels; this is easy to calculate but hard to measure properly (Ingard, 2010).

We can formally compute TL in this context as follows: Take the incident time-averaged power as equal to $\frac{1}{2\rho c} S1$, where the numerator represents the squared-pressure of the incident plane wave of unit amplitude. To find transmitted power, the transmitted pressure amplitude is T, and transmitted acoustic velocity is u equals $\frac{T}{\rho c}$.

Next recall the intensity, $\frac{1}{2} p u^\star$ or pressure times the conjugate of velocity, which in this case equals $\frac{|T|^2}{2\rho c}$; upon multiplying by $S1$ gives the transmitted power. Express the ratio incident to transmitted power in decibels as follows

$$TL = 10 \log_{10} \frac{1}{|T|^2} \tag{10}$$

where to make TL positive to represent more sound reduction, we the inverse ratio is in effect taken.

Now, T can be found directly through above matrix manipulation, or much easier, find R

through the impedance translation theorem and then T via the relation

$$|T|^2 = 1 - |R|^2 \tag{11}$$

which applies to this problem. Note that Eq. (11) is clearly different from the relation $1 + R = T$ which applied to the case of the plane wave reflection coefficient. The key to understanding this difference is that there is no energy loss in this muffler system of Fig. 4. For example the inside of the muffler isn't stuffed with woolly material that absorbs sound energy. This means that the transmitted sound power must equal the incident minus the reflected power.

Equation (10) becomes the formal working definition for computing the performance of the muffler system (take the negative of it to make noise reduction a positive quantity). Fortunately, the muffler performance can be measured in a much simpler way as follows:

$$TL_{measured} = -20 \log_{10} \frac{p_{out}}{p_{in}} \tag{12}$$

where p_{out} and p_{in} are measure pressure quantities, expressed as RMS. Ideally one might get p_{out} with and without the expansion piece, to account for small losses within a tube of constant diameter.
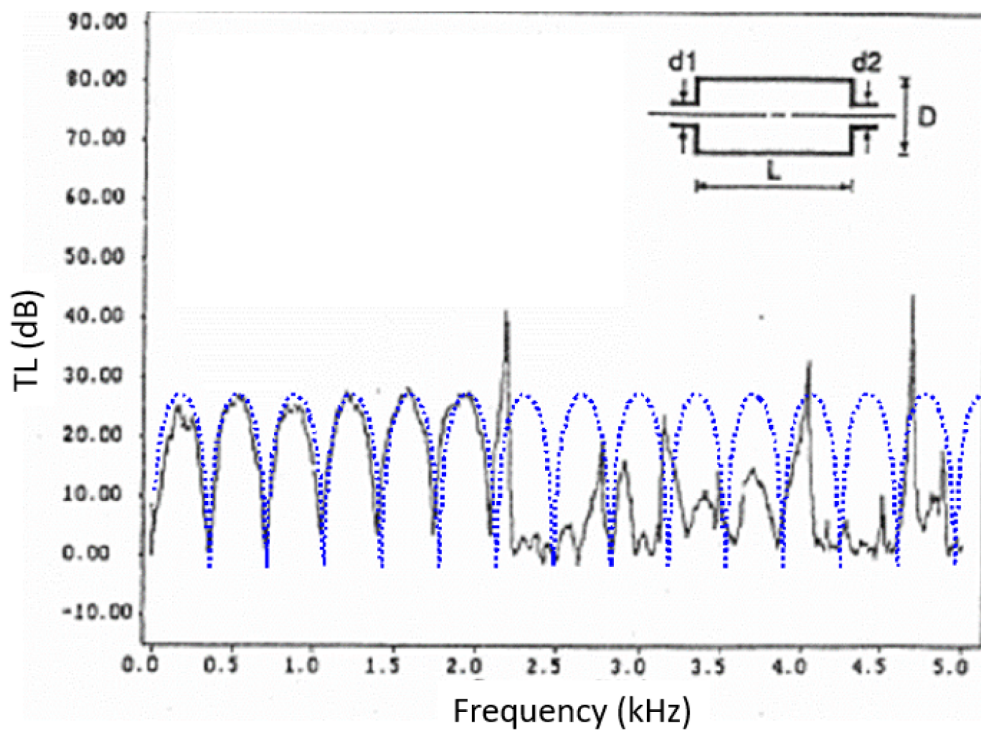

Figure 5: Experimental measurements (black line) by Kim and Kong (1993) for single chamber of $L =$500 mm, chamber diameter $D =$200 mm, and input and output diameters $d1 = d2 =$32 mm, compared with TL based on R as computed with Eq. (11) (blue, dotted line)

A calculation (Fig. 5) of transmission loss for case of $S1 = \pi 0.016^2$ m^2, expansion diameter $S2 = \pi 0.1^2$ m^2 and $L = 0.5$ m is compared with observations made by Kim and Kong (1993), and suggest very large sound reduction (high TL) near 170 Hz and no reduction near 340 Hz, with the pattern continuing. Notice that for frequencies greater than about 2000 Hz (2 kHz) the theory based on Eq. (10) fails because the assumption $f < \frac{c}{1.7d}$ no longer holds.
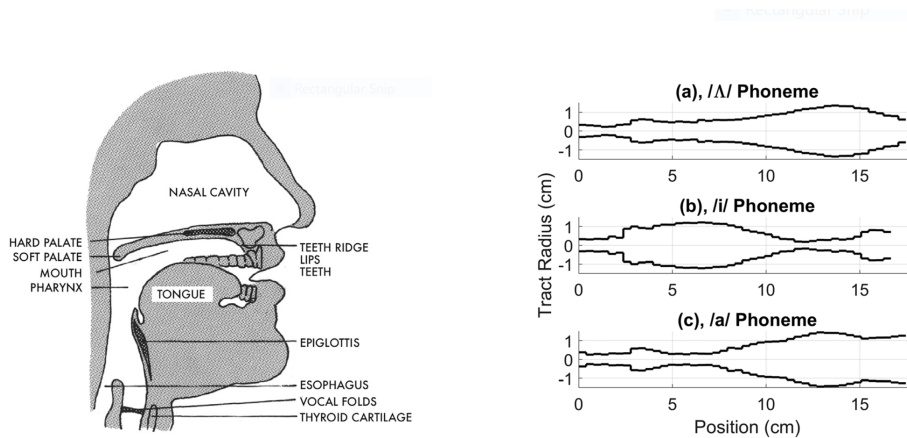
The human vocal tract

Figure 6: left: the human vocal tract (Fig. 1 of Anderson and Sommerfeldt, 2021). Right: model cross sections for human vocal tract for different vowel phonemes (Fig. 4 of of Anderson and Sommerfeldt, 2021)

The Acoustics Research Group at BYU is also known for innovative approaches in graduate acoustics education. For example they demonstrated a really neat problem solved with the impedance translation theorem: the human vocal tract (Fig. 6).

A few models for the vocal tract segmented into short, constant-diameter segments, are shown on the left of Fig. 6, representing different vowel phonemes, or distinct units of sound in English. One can imagine that the simple muffler geometry of Fig. 4 might represent one portion of this model vocal tract, and the impedance translation theorm can be used to connect the effects of the different vocal track segments.

References

Pierce, A. B, *Acoustics, An Introduction to its Physical Principals and Applications*, (Acoustical Society of America, and American Institute of Physics, 1989)

L. M. Brekhovskikh, *Waves in Layered Media*, (Academic Press, New York, 1960)

Y-H Kim and S-W Kong , "Green's solution of the acoustic wave equation for a circular expansion chamber with arbitrary locations of inlet, out outlet port and termination impedance" *J. Acoust. Soc. Am.* 94, July 1993.

B.E. Anderson and S. D. Sommerfeldt , "Solving one-dimensional acoustics systems using the impedance translation theorem and equivalent circuits: A graduate level homework assignment" *J. Acoust. Soc. Am.* 150, December 2021.

ME525 Applied Acoustics Lecture 20, Winter 2024
Solved problems in plane wave reflection, seabed attenuation

Peter H. Dahl, *University of Washington*

Reflection from a halfspace

We'll work through this problem (Fig. 1) for the case without sediment attenuation. View it as a benchmark problem to test your homework solution.
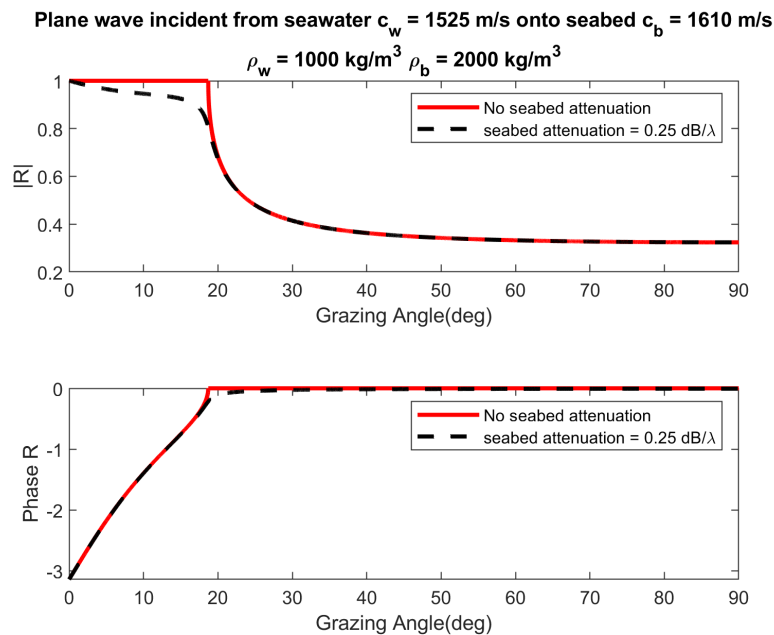

Figure 1: $|R|$ and phase of R as function of grazing angle θ_0 for water-sediment reflection (red lines). The inclusion of sediment attenuation produces the black, dashed lines.

Sediment attenuation is often the key to "everything" in underwater sound, particularly for shallow water geometries for which reflection from seabed is bound to occur. Sediment attenuation will damp out sound as interacts with the seabed, ultimately determining how far sound can travel underwater while reflecting multiple times from the seafloor. There are a multiplicity of ways to express such attenuation, a common approach is to express attenuation as a dB/λ. However to implement the attenuation in reflection problems, one needs to compute the *loss tangent* δ_p from a given dB/λ value (see Jackson and Richardson, 2007)

$$\delta_p = \frac{[\text{dB}/\lambda]\ln(10)}{40\pi}. \tag{1}$$

Having the loss tangent δ_p in hand, then the sound speed of the medium subject to this attenuation,

e.g., c_b, is made complex as follows:

$$c_b \to \frac{c_b}{1 + i\delta_b} \tag{2}$$

Calculation of the reflection coefficient with a complex sound speed in the seabed c_b based on 0.25 dB/λ (typical value) is shown by black, dashed line in Fig. 1. At first look the effect appears small, however observe that for angles less than the critical angle for which we would anticipate total reflection or $|R| = 1$ now assume a small reduction in amplitude. This has a huge, cumulative effect after several reflections from the seafloor.

Another way of expressing attenuation is by way the parameter Q which is often seen in seismology. A "high Q" media means low attenuation. A handy relation is

$$\text{dB}/\lambda \approx 27Q^{-1} \tag{3}$$

Reflection from a layered media using the Impedance Translation Theorem

We'll work through a couple of problems involving the Impedance Translation Theorem and layered (Figs. 2 and 3). Again view for these cases without sediment attenuation to serve as benchmark problems to test your homework solution. Importantly, note that the acoustic frequency enters the problem. There is length scale and the layer thickness L of 100 m, depending on frequency may appear acoustically as a "thick layer" relative to the acoustic wavelength λ, as "thin layer", or if $\lambda \gg L$, may not be observable at all in the calculations. As in Fig. 1 the calculations are repeated with some sediment attenuation.
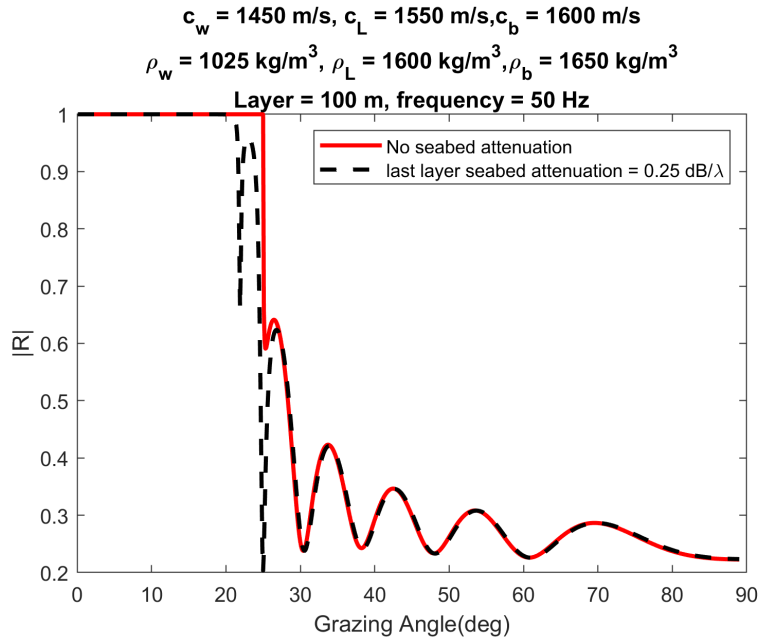
Figure 2: Magnitude of the plane reflection coefficient $|R|$ from a layered seabed as function of grazing angle (red line); inclusion of sediment attenuation produces the black, dashed line.
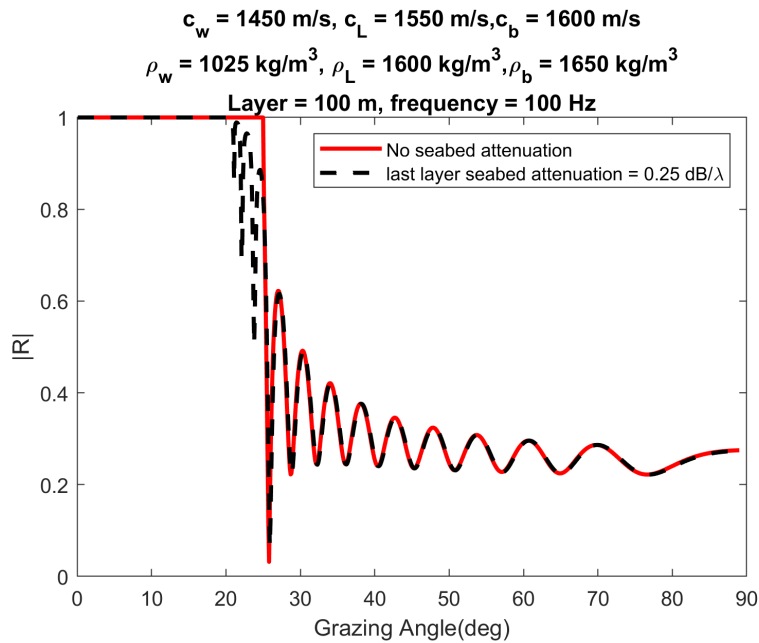

Figure 3: Magnitude of the plane reflection coefficient $|R|$ from a layered seabed as function of grazing angle; inclusion of sediment attenuation produces the black, dashed line.

Example closer to current research: sound propagation over mud-like sediments

The following example remains somewhat idealized nonetheless serves as a notional working model for plane wave reflection from a mud-like sediment of thickness 9 m. Such conditions are

approximately in effect in waters about 100 km south of Cape Cod (depth $\sim$ 75 m) known as the New England Mud Patch (NEMP). A key characteristic of the NEMP is the mud layer of thickness of order 10 m, where the sound speed (and density) are less than water. Notice the profound (theoretical) difference on how sound interacts with this seabed at a frequency of 2000 Hz versus 20 Hz.
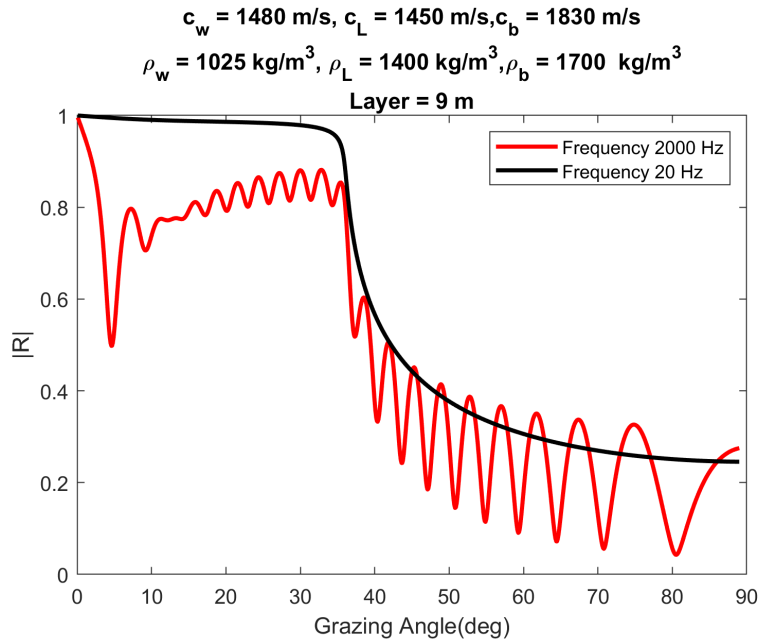

Figure 4: Magnitude of the plane reflection coefficient $|R|$ from a mud-like sediment off the coast of New England. Attenuation for each case is 0.25 dB/λ and two frequencies are shown.

References

L. M. Brekhovskikh, *Waves in Layered Media*, (Academic Press, New York, 1960)
D.R. Jackson and M. Richardson. *High-Frequency Seafloor Acoustics*, (Springer, New York, 2007)
Frisk, G. V. *Ocean and Seabed Acoustics* (Prentice Hall, Englewood Cliffs, NJ, 1994)